Species-specific differences in follicular antral sizes result from diffusion-based limitations on the thickness of the granulosa cell layer

Molecular Human Reproduction, Vol.20, No.3 pp. 208–221, 2014
Advanced Access publication on November 11, 2013 doi:10.1093/molehr/gat078

molecular human reproduction
MHR | basic science of reproductive medicine

ORIGINAL RESEARCH

Species-specific differences in follicular antral sizes result from diffusion-based limitations on the thickness of the granulosa cell layer

M. Bächler[1,†], D. Menshykau[1,2,†], Ch. De Geyter[3], and D. Iber[1,2,*]

[1]Department for Biosystems, Science, and Engineering (D-BSSE), ETH Zürich, Mattenstraße 26, Basel 4058, Basel, Switzerland [2]Swiss Institute of Bioinformatics, Switzerland [3]Clinic of Gynecological Endocrinology and Reproductive Medicine, Women's Hospital, University of Basel, Basel, Switzerland

*Correspondence address. Tel: +41-61-387-3210; Fax: +41-61-387-31-94; E-mail: dagmar.iber@bsse.ethz.ch

Submitted on September 7, 2013; resubmitted on October 26, 2013; accepted on November 4, 2013

ABSTRACT: The size of mature oocytes is similar across mammalian species, yet the size of ovarian follicles increases with species size, with some ovarian follicles reaching diameters >1000-fold the size of the enclosed oocyte. Here we show that the different follicular sizes can be explained with diffusion-based limitations on the thickness of the hormone-secreting granulosa layer. By analysing published data on human follicular growth and granulosa cell expansion during follicular maturation we find that the 4-fold increase of the antral follicle diameter is entirely driven by an increase in the follicular fluid volume, while the thickness of the surrounding granulosa layer remains constant at $\sim 45 \pm 10$ μm. Based on the measured kinetic constants, the model reveals that the observed fall in the gonadotrophin concentration from peripheral blood circulation to the follicular antrum is a result of sequestration in the granulosa. The model further shows that as a result of sequestration, an increased granulosa thickness cannot substantially increase estradiol production but rather deprives the oocyte from gonadotrophins. Larger animals (with a larger blood volume) require more estradiol as produced by the ovaries to down-regulate follicle-stimulating hormone-secretion in the pituitary. Larger follicle diameters result in larger follicle surface areas for constant granulosa layer thickness. The reported increase in the follicular surface area in larger species indeed correlates linearly both with species mass and with the predicted increase in estradiol output. In summary, we propose a structural role for the antrum in that it determines the volume of the granulosa layer and thus the level of estrogen production.

Key words: human follicle development / scaling / gradients / gonadotrophins / computational modelling

Introduction

Ovarian follicle development has been studied for decades and has enabled major progress in animal breeding and in human reproductive medicine (Richards and Pangas, 2010; Adams *et al.*, 2012). The overall process appears to be similar across mammals: during menstruation, increased secretion of follicle-stimulating hormone (FSH) in the pituitary promotes the recruitment of a new cohort of growing follicles in the ovaries. FSH and luteinizing hormone (LH) are both transported via the blood circulation to the theca (Richards and Pangas, 2010) (Fig. 1A and B), and stimulate there the production of androgens, which are converted to estrogens in the granulosa cell layer of the follicle (Erickson *et al.*, 1979; Bao and Garverick, 1998; Silva and Price, 2002). The estrogens, in turn, enter the blood and down-regulate the production and secretion of FSH in the pituitary (Kumar *et al.*, 1997). As the FSH concentration in the blood circulation subsequently falls, an increasing number of follicles undergoes atresia, and only the one follicle that can best compensate the lower FSH signalling with LH signalling survives and becomes the dominant, ovulating follicle (Xu *et al.*, 1995).

While the size of mature oocytes is similar across different mammalian species, the size of ovarian follicles differs greatly (Table I), with some ovarian follicles reaching diameters >1000-fold the size of the oocyte that develops inside (Gosden and Telfer, 1987). Larger follicles are mainly characterized by a larger size of the fluid-filled cavity, the antrum. No direct role of the antrum in follicular function has so far been identified and it is an open question why the size of the antrum (and thus that of the follicle) is so variable among species. The follicular fluid that fills the antral cavity contains water, electrolytes, serum proteins and high concentrations of steroid hormones secreted by the surrounding granulosa cells (Rodgers and Irving-Rodgers, 2010). The membrana granulosa of

[†] These authors contributed equally.

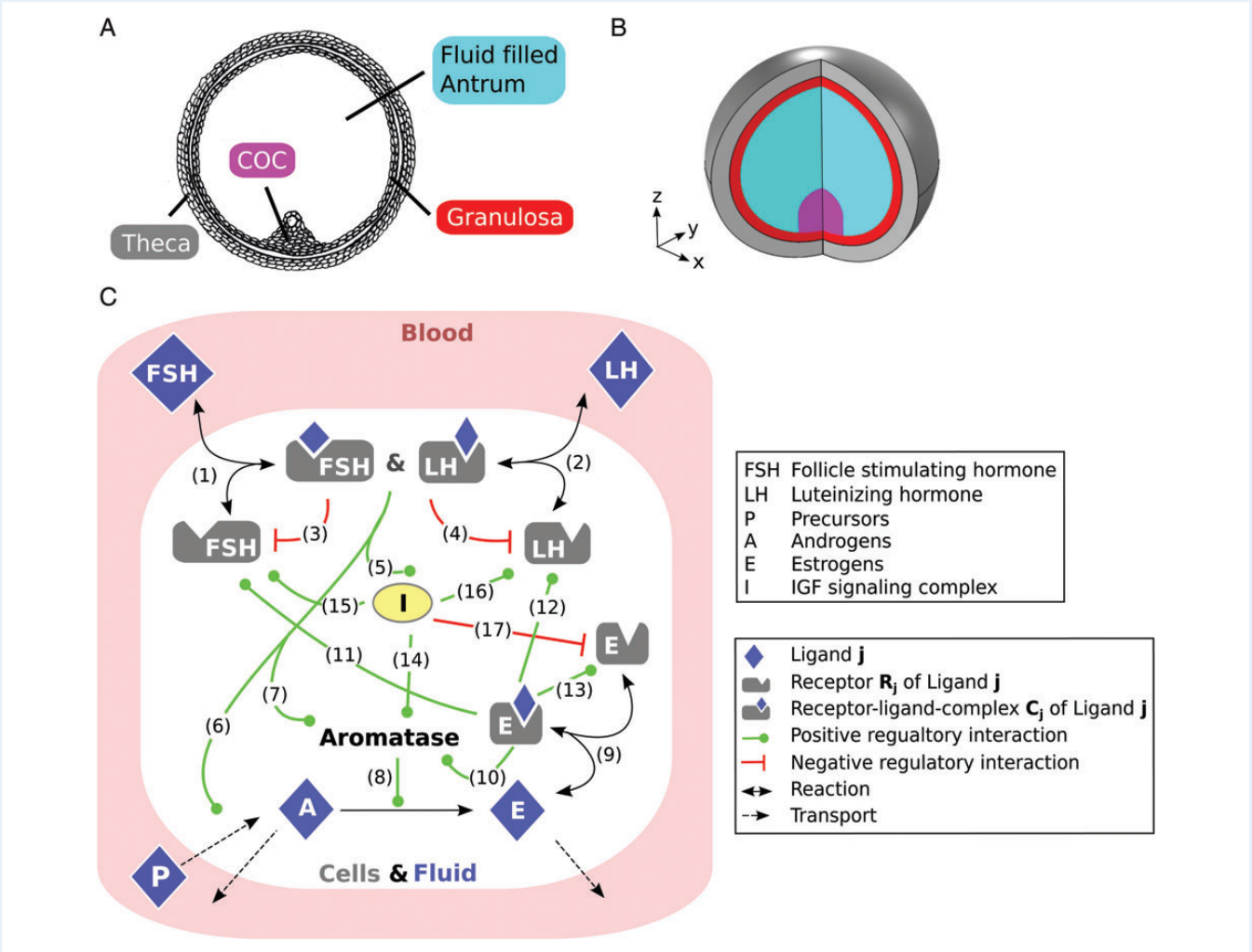

Figure 1 A graphical summary of the model for ovarian follicle development. (**A**) A schematic 2D representation of an ovarian follicle. The follicle is a multilayered structure. Inside the follicle is the fluid-filled antrum, which is surrounded by a granulosa cell layer. The outer layer, the theca, is innervated by a mesh of capillary blood vessels. All other parts of the follicle are avascular. The oocyte together with the surrounding cumulus cells forms the COC. The COC lies on one side of the follicle and is attached to the granulosa cell layer. (**B**) A schematic view of the 3D computational domain for the follicle. Compartments are coloured as in (A). Note that the proportions of the compartments have been changed for better visualization. (**C**) The modelled signalling network for the regulation of follicular development, including FSH, LH, estrogens [E], androgens [A] and IGF [I] signalling. Receptors and ligand–receptor complexes of component j are indicated as R_j and C_j, respectively. Black dotted arrows indicate exchange with the blood, black solid arrows chemical reactions (binding or catalysis), green arrows positive regulatory interactions, while red arrows indicate negative regulatory interactions. All components also decay, but for greater clarity decay reactions have not been included in the scheme. For a more detailed discussion of the reaction network along with the evidence see the main text; numbers in brackets refer to single reactions as called out in the main text.

the follicle is avascular and can therefore only be reached by diffusion from the vascularized theca (Fig. 1A and B). The oocyte together with the surrounding cumulus cells forms the cumulus–oocyte complex (COC). The COC resides eccentrically in the follicle and is attached to the granulosa cell layer.

The geometry, the timing of the maturation process and the core regulatory network that controls the follicle maturation process have been defined (Richards and Pangas, 2010). Within the ovarian follicle, FSH and LH regulate a large number of target genes and proteins, which interact in a complex regulatory network (Gloaguen *et al.*, 2011). Within the follicle, the most important regulatory factors are steroid hormones (androgens and estrogens) but also insulin-like hormones, as summarized in Fig. 1C. The regulatory network is further complicated by the spatial restriction of many of the gene expression domains. Thus, many of the signalling components are produced only in parts of the follicle, with some diffusing and others being cell-bound within the tissue.

Computational models have the potential to integrate large amounts of published information and can be used to evaluate the consistency of available data. A number of computational models have previously been developed to analyse aspects of the follicle maturation process (for a review, see (Vetharaniam *et al.*, 2010), but only few models explore the processes within the follicle itself. We have recently developed a

Table I The diameter of the mature follicle and characteristic weight in different mammalian species.

Follicle (mm)	Weight (kg)	Species	Ref.
0.42	0.03	Mouse	Griffin et al. (2006)
0.55	0.2–0.25	Albino rat	Sangha and Guraya (1989)
0.64	0.2	Hamster	Griffin et al. (2006)
2.8	2.7	Rabbit	Osteen and Mills (1980)
4	3	Cat	Izumi et al. (2012)
6	9–10	Beagle (dog)	Reynaud et al. (2009)
6	23	Sheep	Aurich(2011)
7.5	35	Serrana goat	Simões et al. (2006)
8	150	Gilt	Chiou et al. (2004)
7–12	48–84	Alpaca	Bravo et al. (1991)
7–12	130–200	Llama	Bravo et al. (1991)
16	250–800	Water buffalo	Taneja et al. (1996)
20	700	Cow	Evans (2003)
20	2700	Elephant	Lueders et al. (2011)
23	60	Human	Evans (2003)
20–25	800	Summatran rhinoceros	Hermes et al. (2007)
27–38	300–550	Camel dromedarius	Manjunatha et al. (2012)
30–34	1800	White rhinoceros	Hermes et al. (2007)
50	1000	Black rhinoceros	Hermes et al. (2007)
55	450	Horse	Aurich (2011)
120	1900	Indian rhinoceros	Hermes et al. (2007)

model for the spatiotemporal signalling dynamics of the core regulatory network during bovine folliculogenesis (Iber and De Geyter, 2013). The model was solved on a 1D-domain and demonstrated that the observed bovine gene expression patterns can indeed result from these core regulatory interactions. The time-dependent 3D-geometry of the human follicle and the rate of cellular expansion have been measured in great detail during the maturation process (McNatty, 1981; Gougeon, 1986). Recently, the gene expression levels have also been measured in human follicles at various stages of their development (Jeppesen et al., 2012). Given the availability of these quantitative data sets, it is now feasible to construct a 3D-computational model for the human follicle maturation process. To this end, we extended the bovine model to human folliculogenesis using published quantitative human data on follicle growth, cell expansion, hormone concentrations and gene expression kinetics. Based on detailed quantitative growth data, the granulosa layer retains a constant thickness of ~45 μm during follicular growth, even though granulosa cells proliferate strongly. Thus, the massive expansion of the follicle from a diameter of 0.5–2 cm within 10–14 days of development is driven entirely by an increase in the volume of the follicular fluid. Based on the measured kinetic constants, the model further predicts that the granulosa cell layer would sequester hormones and that this would result in a concentration difference between the serum and the follicular fluid. The predicted concentration differences have been noted previously (Stone et al., 1988) and we confirmed in measurements that model predictions and experiments agree quantitatively for a range of serum concentrations. We subsequently used the validated model to test the impact of altering either the size of the follicle or the thickness of the granulosa cell layer, and we find that, because of the diffusion limitations, estradiol production can rise substantially only by increasing the size of the follicle and thus the surface of the granulosa cell layer. We propose the diffusion limitations across the granulosa cell layer as the reason for the follicular expansion in larger animals.

Materials and Methods

The model

Folliculogenesis in cattle and humans bears great similarity (Aerts and Bols, 2010). We therefore based the model for human folliculogenesis on our previous work on bovine folliculogenesis (Iber and De Geyter, 2013). The model is formulated as isotropic advection–reaction–diffusion equations for a compound c_i with diffusion coefficient D_i and external velocity field u

$$\partial_t \boldsymbol{c_i} + \nabla(\boldsymbol{u c_i}) = \boldsymbol{D_i}\nabla^2 \boldsymbol{c_i} + \mathrm{R}(\boldsymbol{c_i}) \qquad (1)$$

$R(c_i)$ denotes the reaction terms that describe the regulatory interactions of the hormones FSH (F), LH (L) and their receptors, of androgens (A), estradiol (E) and the estradiol receptor for steroid-dependent signalling, as well as of IGF signalling (I) as shown in Fig. 1C. The reaction terms $R(c_i)$ are listed in the Supplementary data. Much as in the bovine model we use zero flux boundary conditions for all hormones, receptors and their complexes. The parameter values are listed in Supplementary data, Table SI.

Simulations

The PDEs were solved with finite element methods as implemented in COMSOL Multiphysics 4.3a. COMSOL Multiphysics is a well-established software package and several studies confirm that COMSOL provides accurate solutions to reaction–diffusion equations both on constant (Cutress et al., 2010) and growing domains (Carin, 2006; Thummler and Weddemann, 2007; Weddemann and Thummler, 2008). Simulations on growing domains were carried out using the Arbitrary Lagrangian–Eulerian method. Details on how biological models in general and reaction–diffusion–advection equations on a domain comprising several subdomains in particular are implemented in COMSOL have been described by us previously (Germann et al., 2011; Menshykau and Iber, 2012). The accuracy of the calculation for the components with sharpest concentration profiles (FSHR and LHR) was 2% or higher, except for a narrow range of time where the accuracy was 8% or higher.

Measurements of the concentrations of FSH, LH and hCG

In eight women treated with exogenous gonadotrophins for ovarian hyperstimulation in assisted reproduction the follicular fluid of the first ovarian follicle in the right and in the left ovary were collected together with serum for the measurement of the concentrations of FSH, LH and hCG, respectively. The gonadotrophin levels both in the serum and in the follicular fluid were measured by quantitative determination using the Elecsys System, Roche Diagnostics, Rotkreuz, Switzerland. All participants were informed about the rationale of the project and signed informed consent.

Results

The growth of human ovarian follicles

Detailed quantitative data sets on the growth of human follicles and on the expansion of the different compartments are available. The thickness of the granulosa cell layer and the follicular volume are the most important compartments in our model and detailed knowledge of their expansion (McNatty, 1981; Gougeon, 1986) allows us to simulate the regulatory network on a three-dimensional axisymmetric follicular domain (Fig. 1B) with realistic tissue layer sizes rather than on an idealized, linearly expanding 1D-domain, as was the case in our previous bovine model (Iber and De Geyter, 2013). The thickness of the theca and the size of the COC have not been reported over time. However, the exact thickness of the theca does not impact on our model predictions because the theca is vascularized by blood capillaries. Therefore, the hormone concentrations in this layer are considered to directly reflect the serum hormone concentrations and not to be affected significantly by reaction and diffusion processes in this layer. In line with previous reports we will use 100 μm for the thickness of the theca throughout follicular development (Singh and Adams, 2000). The diameter of the mature COC at ovulation is ~3 mm. While the COC is well known to expand during follicle maturation we have not found detailed size measurements at earlier stages, and we therefore assume that the diameter of the COC expands at a similar rate as that of the follicle.

The pre-ovulatory phase starts at a follicle diameter of around 5 mm and ends after around 14 days at 25 mm (Gougeon, 1986). The growth rate remains grossly constant which implies $v_F = 1.74 \times 10^{-5}$ mm s^{-1} as the growth rate of the follicle diameter. Both the volume of the follicular fluid (Fig. 2A) and the number of granulosa cells (Fig. 2B) have been reported for the entire pre-ovulatory phase (Gougeon, 1986; McNatty, 1981). The follicle is about spherical (Fig. 1A and B) and we can therefore use the relation $V_{FF} = 4/3\pi r_{FF}^3$ to convert the follicular fluid volume V_{FF} into the radius of the follicular fluid compartment, r_{FF} (Fig. 2C). We note that the radius and follicular volume obtained with such a spherical approximation are very close to the measured data [compare measurements (dots) and spherical approximation (solid lines) in Fig. 2A and C]. The volume of human ovarian granulosa cells has been determined as $V_C = 1140$ μm^3 (Dhar *et al.*, 1996). By multiplying the number of granulosa cells with the cell volume we obtain the volume of the granulosa layer. Using again the spherical shape of the follicle we note that the volume of the granulosa layer is $V_G = 4/3\pi(r_G^3 - r_{FF}^3)$, where $r_G = r_F + s_G$ is the combined radius of follicular fluid and granulosa layer and s_G is the thickness of the granulosa layer. We can thus calculate the thickness s_G of the granulosa layer at different follicle sizes and find that the granulosa thickness is 45 ± 10 μm throughout follicular development (Fig. 2D). Finally we can use the growth rate v_F to relate the follicle diameter to developmental time (Fig. 2E and F). Again we stress that the approximations fit the measured data very well as evident by comparing the measurements (dots) and spherical approximation (solid lines) in Fig. 2A–F.

The conversion of the measured diameters and cell numbers and volumes permits us to approximate the radii of the different compartments in our simulations over time (Fig. 2G). The growth kinetics are described by six parameter values, as listed in Supplementary data, Table SI. The geometry of the follicle used for modelling the 3D-follicle (Fig. 1B) has a rotational axis of symmetry going through the centre of follicle and the centre of COC (Fig. 2H). It should be noted that only the follicular fluid and the COC layers expand at speed v_F; the thickness of the thecal and granulosa cell layers do not change over time (Fig. 2D and F) and the end-points are thus only shifted as the follicular fluid and COC expand together (Fig. 2G). The final diameter of the COC is 3 mm in the model.

A model for human folliculogenesis

Building on our model for bovine folliculogenesis (Iber and De Geyter, 2013), we next sought to develop a model for the regulatory network that controls the development of the dominant human ovarian follicle in the pre-ovulatory phase, aiming at integrating the known core regulatory interactions into a consistent framework. We formulated the model as a set of isotropic advection–reaction–diffusion equations that describe the regulatory interactions of the hormones FSH (*F*), LH (*L*), androgens (*A*) and estradiol (*E*) as well as of IGF signalling (*I*). The ligands can diffuse inside the entire follicle, while their receptors are restricted to cells, thus diffuse at much lower speeds (Supplementary data, Table SI) and cannot diffuse between the different tissue layers or in the follicular fluid (Fig. 1A and B). Previous studies have successfully described the *in vivo* distribution of diffusible signalling molecules with continuous reaction–diffusion equations on a domain with a length scale as small as 10 cells (Iber and Zeller, 2012), and we therefore expect that the ligands in our model can also be adequately described by continuous reaction–diffusion equations. The receptors are more of a concern as these are restricted to cells and their diffusion is thus limited by the cell boundaries in the tissue. We have previously noted that during the receptor half-life receptors can diffuse over distances of less than the diameter of one epithelial cell (Menshykau *et al.*, 2012). For simplicity, we therefore also use continuous reaction–diffusion equations for the receptors.

The modelled core network regulating the development of the follicle is shown in Fig. 1C and the reaction terms are listed in the Supplementary data. In the mathematical formulation we consider four types of reactions: complex formation at rate k_{on} and complex dissolution at rate k_{off}, linear decay at rate $\delta\, c_i$, where c_i refers to the concentration of the component *i*, and production at a constant rate ρ or at a modulated rate $\rho\, f(\sigma(c_i, K_i))$. Here the σ term indicates a Hill function:

$$\sigma_i = \frac{c_i^n}{c_i^n + K_i^n},$$

with Hill constant K_i, which specifies the concentration of c_i where half-maximal activity is observed, and Hill coefficient n which defines the steepness of the response; we are using $n = 2$ throughout. The Hill functions can be used in different combinations to either specify activating influences, or by using $1 - \sigma_i$ for inhibitory impacts of c_i. The regulatory interactions along with the evidence have been discussed previously (Iber and De Geyter, 2013). In brief, the following regulatory interactions are included in the model: FSH and LH, secreted by the pituitary gland and transported through the blood, move through the endothelium and subendothelial basal lamina of the thecal vasculature into the thecal layer of the follicle (Rodgers and Irving-Rodgers, 2010) and bind their receptors to form FSH and LH receptor ligand complexes (Fig. 1C, arrows (abbreviated as A# in the following) 1 and 2). *FSH receptor* is constitutively expressed in granulosa and COC and its expression can be induced by

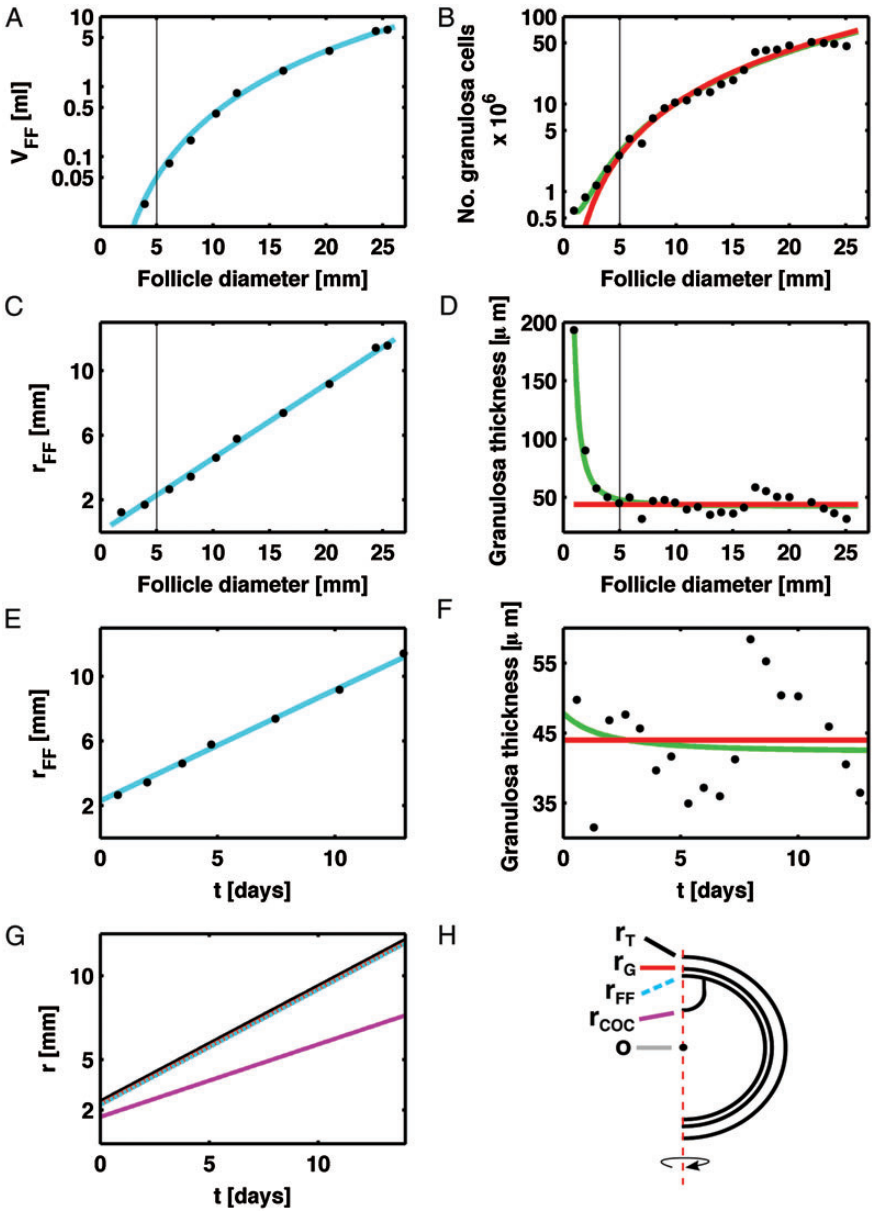

Figure 2 Follicular growth. (**A**) The volume of the follicular fluid at different follicle diameters d_F. The data (dots) was reproduced from McNatty (1981). The line shows the follicular fluid volume obtained with $V_{FF} = 4/3\pi r_{FF}^3$ where r_{FF} was obtained by fitting the converted data points in (**C**) by a straight line. (**B**) The number of granulosa cells in human Graafian follicles at different follicle diameters d_F. The data (dots) was reproduced from (McNatty, 1981). The lines show the number of granulosa cells when converting the granulosa thickness, $s_G = r_G - r_{FF}$, that is obtained in (**D**) back into the number of granulosa cells $N_G = V_G/V_C$, where $V_G = 4/3\pi(r_G^3 - r_{FF}^3)$ is the granulosa layer volume and $V_C = 1140\ \mu m^3$ is the measured granulosa cell volume. The green line represents the predicted granulosa cell number based on a polynomial fit, while the red line is based on a linear fit in (**F**). (C) The radius of the follicular fluid as obtained by fitting the converted volume data in (A) using the relation $V_{FF} = 4/3\pi r_{FF}^3$. (D) The granulosa layer thickness s_G in human Graafian follicles at different follicle diameters obtained by conversion of the data in (B). The thickness was calculated by determining the granulosa volume $V_G = N_G \times V_C$ as the product of granulosa cell number N_G and cell volume $V_C = 1140\ \mu m^3$. The granulosa thickness $s_G = r_G - r_{FF} = 44\ \mu m$ was then obtained from $V_G = 4/3\pi s_G^3$. The green line represents a polynomial fit to the data, while the red line represents a linear fit to the data. (**E**) The radius of the follicular fluid and (F) the thickness of the granulosa layer versus developmental time as obtained by converting follicle diameter in (C) and (D) using $d_F = 5\ mm + v_F t$. (**G**) The radii of the different compartments over simulation time. The radius r_{FF} represents the radius of the fluid filled cavity (dotted cyan line). The radius $r_{COC} = r_{FF} - d_{COC}$ defines the start of the COC domain (magenta line); d_{COC} is the diameter of the COC. The radius of the sphere that includes both follicular fluid and granulosa cells layer has radius $r_G = s_G + r_{FF}$ (red line), where s_G is the thickness of the granulosa layer. The outer delimiter of the follicle is given by the radius $r_T = r_G + s_T$ (black line), where s_T is the thickness of the thecal tissue. (**H**) A section along the axis of symmetry of the 3D computational domain, shown in Fig. 1B.

signalling interactions in all tissue layers. FSH- and LH-signalling reduces the stability of the FSH and LH receptor mRNA (A3, A4) (Schwall and Erickson, 1984; Themmen *et al.*, 1991; Nair *et al.*, 2002), supports IGF signalling (A5) and enhances the production of androgens (A6) (Bao and Garverick, 1998), as well as the production and activity of aromatase (A7) (Erickson *et al.*, 1979; Silva and Price, 2002), the enzyme that catalyses androgens into estrogens (A8). Production of androgens is restricted to the theca, while its conversion to estrogens is restricted to granulosa and COC. Estrogens bind to their receptors, forming estrogen receptor–ligand complexes (A9). Estrogen signalling enhances the production of aromatase (A10), as well as the production of the receptors for FSH (A11), LH (A12) and estradiol (A13) (Richards, 1975; Sharma *et al.*, 1999; Couse *et al.*, 2005). IGF signalling is necessary for the gonadotrophin-dependent expression of *aromatase* (A14) (Silva and Price, 2002), enhances the production of FSH and LH receptors (A15, A16) (Hirakawa *et al.*, 1999; Minegishi *et al.*, 2000) and reduces *estrogen receptor beta* expression (A17). We aimed at developing a parsimonious model with the simplest possible set of regulatory interactions that reproduce the measurements. Aromatase is therefore not explicitly included because its activity can well be approximated as the direct result of IGF signalling and of the regulation through FSH and LH.

The reaction terms are identical to those used in the bovine model (Iber and De Geyter, 2013) except for two new regulatory interactions that had to be added to the human model to account for a marked difference in the bovine and human gene expression data. Thus, in the human granulosa cells *FSH-receptor* expression is high in small follicles (6 mm) and subsequently decreases (Jeppesen *et al.*, 2012), whereas in bovine follicles *FSH-receptor* expression is lower and increases during follicular growth (Xu *et al.*, 1995; Bao and Garverick, 1998). To account for this difference we needed to introduce a previously neglected negative feedback of gonadotrophin signalling on *FSH-* and *LH-receptor* expression (Fig. 1C, A3,A4) and increase the rate of FSH/LH/estradiol-independent *FSH-receptor* expression, as described in the Supplementary data.

We initiate the model without any hormones, receptors and hormone–receptor complexes, because we want to study the mechanisms that result in the emergence of the characteristic gene expression patterns in the follicle. We note that other homogenous initial conditions within the physiological range do not affect our model predictions. The only exception is the initial concentration of the IGF–signalling complex in the theca, which is important to reproduce the early expression of *LH receptors* in the theca.

Model consistency with human data

Even though the model has 35 kinetic parameters and 6 growth parameters it is very well constrained (Supplementary data, Table SI). We discussed the data-based derivation of the growth parameters in the previous section. The first 26 kinetic parameter values in Supplementary data, Table SI are the same as in the bovine model and all but two of these parameter values have been directly measured, sometimes in several independent experiments; two parameter values were previously established in the bovine model based on gene expression data (Iber and De Geyter, 2013). The remaining seven parameter values had to be changed to account for the differences in the measured gene expression time courses and steroid concentrations in women and cattle. Thus, the androgen concentration is higher in human than in bovine follicles, whereas the estradiol concentration is lower (Xu *et al.*, 1995; Bao and Garverick, 1998; Jeppesen *et al.*, 2012). The reported human concentration ranges are shown in Fig. 3A as shadings. To reproduce the human follicular androgen concentration the androgen production rate ρ_A had

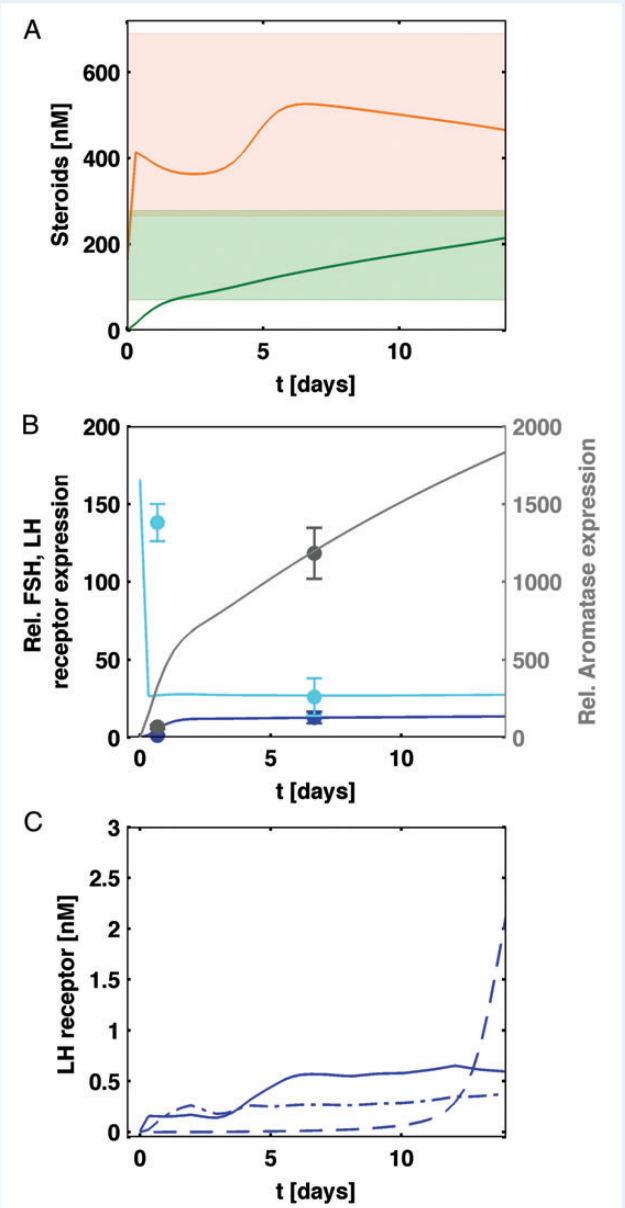

Figure 3 Model consistency with human data. (**A**) The measured (shaded areas) and simulated (lines) steroid concentrations of androgens (orange line and shading) and estradiol (green line and shading) in the follicular fluid over time. The data were recorded by (Jeppesen *et al.*, 2012). (**B**) Data (markers) and simulation output (lines) of the relative expression of *FSH-receptor* (cyan), *LH-receptor* (blue) and aromatase (grey) in the granulosa over developmental time. The data were recorded by (Jeppesen *et al.*, 2012) for follicles of different diameters. Data were converted from diameter into time by using the relation $d_F = 5\ \text{mm} + v_F t$. The vertical axis shows mRNA expression levels normalized to *Gapdh* expression. (**C**) The predicted maximal concentration of the LH receptor in theca (solid), granulosa (dash-dotted) and COC (dashed line) over developmental time.

to be increased 4-fold. To reproduce the measured human estrogen concentration the Hill constant for IGF-dependent regulatory processes, K_I, had to be lowered. The *FSH-receptor* expression has been found to decrease over time (Jeppesen *et al.*, 2012). The LH and FSH receptor mRNAs have previously been reported to be destabilized in response to gonadotrophin receptor-dependent signalling (Schwall and Erickson, 1984; Themmen *et al.*, 1991; Nair *et al.*, 2002). To achieve such a negative feedback (Fig. 1C, arrows 3,4) the signalling threshold K_F had to be lowered (Fig. 3B). Since both FSH- and LH receptors are G-protein-coupled receptors that link to the same signalling machinery (Richards *et al.*, 2002; Wood and Strauss, 2002) we now use equal thresholds for FSH and LH signalling, i.e. $K_L = K_F$. To still obtain similar *LH-receptor* expression levels we had to increase the production rate for the IGF receptor complex, ρ_I, some 5-fold. Finally, there is an FSH/LH/estrogen-independent regulation of *FSH-receptor* expression in granulosa and COC (Zhou *et al.*, 1997; Couse *et al.*, 2005), which we assume has a constant activity ϑ_G and ϑ_{COC}. This value had to be increased in the granulosa to achieve a high initial rate of *FSH-receptor* expression that can then decrease as a result of the negative feedback (Fig. 3B). The activity in the COC, ϑ_{COC}, had to be lowered to limit the total receptor concentration to a physiologically realistic range. With these changes, the measured gene expression rates for *FSH-* and *LH receptors* as well as for aromatase are well reproduced (Fig. 3B) and the total LH receptor concentration remains <3 nM (Fig. 3C) as measured in experiments (Erickson *et al.*, 1979).

Spatiotemporal dynamics of the regulatory network in the follicle

With the model and parameters all set we first simulated the physiological situation of follicle maturation in healthy women. The human serum levels of FSH and LH change during the menstrual cycle (Brindle *et al.*, 2006) and we used the measured FSH and LH concentrations as the thecal gonadotrophin concentrations (Fig. 4A and B). The simulations show how the hormones enter the follicle from the theca by diffusion and how the concentration increases slowly inside the follicle (Fig. 4C and D). Interestingly, also the final hormone concentrations in the follicular fluid are much lower than in the serum (Fig. 4C and D). This is the result of hormone sequestration in the membrana granulosa by receptor binding (Fig. 4E and F). We notice that most FSH is bound in the granulosa layer (Fig. 4E), while most LH is bound in the theca (Fig. 4F), and some less in the granulosa (Fig. 4F). These distributions are also in good agreement with the reported expression patterns of *FSH-* and *LH receptors* (Fig. 4G and H). Thus, *FSH receptors* are mainly expressed in the membrane granulosa (Rhind *et al.*, 1992), while *LH receptors* are initially expressed mainly in the theca and later also in the granulosa (Xu *et al.*, 1995; Bao and Garverick, 1998). As a result of hormone sequestration, little FSH and LH reaches the COC (Fig. 4E and F) and little receptor is expressed, which agrees well with the measured low receptor expression rates in the COC (Eppig *et al.*, 1997; Assou *et al.*, 2006; Jeppesen *et al.*, 2012). In the follicular fluid, hormones have a uniform concentration because they are mixed rapidly when compared with the time scale of development due to convection with moving fluid (Fig. 4C and D).

Sensitivity to parameter values and initial conditions

While the parameter values are all based on experimental measurements (Supplementary data, Table SI), these measurements were carried out in a range of different systems and may suffer from experimental errors and inaccuracies. We therefore checked the robustness of the observed concentration difference between serum and follicular fluid to changes in the parameter values. To that end we re-simulated our model with parameter values that were drawn from a Gaussian distribution with a mean value as given in Supplementary data, Table SI and relative standard deviation of 0.1. The standard deviation of the simulations at the final time point (Day 14, depicted as grey shadow in Fig. 4C–F) demonstrates little impact of such deviations in the parameter values on the relative FSH and LH concentrations between serum and follicular fluid (Fig. 4C and D). We, however, noted considerable variance in the extent to which FSH- or LH-bound receptor complexes emerge in the theca (Fig. 4E and F).

To identify the parameters with the largest impact on the relative gonadotrophin concentration in the follicular fluid and serum we carried out a sensitivity analysis. Here we calculated the relative change in the FSH concentration ratio in the two compartments in response to a 1% change in the parameter values p_i, i.e.

$$S = \frac{\Delta \text{Ratio}/\text{ratio}}{\Delta p_i / p_i}.$$

Figure 5 includes all parameters for which $S > 0.001$. We note that the largest impact is observed for the gonadotrophin diffusion coefficient D_H, the FSH receptor production rates ρ_{FR}, ρ_{FRG} and ρ_{FRcoc}, the decay rate of the FSH–receptor complex δ_{FRc}, and the FSH response threshold K_{FR}. This further supports the observation that the gonadotrophin concentration difference between serum and follicular fluid results from receptor-dependent sequestration in the theca and granulosa (Fig. 4E and F). The initial conditions on the other hand have little impact, as long as they are homogenous in space.

Concentration differences between the serum and the follicular fluid as a result of hormone sequestration in the granulosa cell layer

The predicted concentration differences between serum and follicular fluid are evident already in 25-year-old published data (Stone *et al.*, 1988). However, since these concentration differences have received no prior attention and are central to the predictions of the present model, we sought to confirm these concentration differences between serum and follicular fluid by measuring the FSH, LH and hCG concentrations in women. Thus, we assayed the hormone concentrations in the first aspirated left and right follicle of eight infertile patients undergoing oocyte retrieval for assisted reproduction and in their serum. These patients were treated with exogenous human menopausal gonadotrophins or with recombinant FSH and had received one single subcutaneous bolus injection of human urinary chorionic gonadotrophin (hCG) for ovulation induction, a substitute for LH with a longer serum half-life, but with a receptor-dependent turn-over rate of hCG similar to that of LH (Nakamura *et al.*, 2000). To compare the measured values to the simulations we converted the reported IU/l units into SI units using the following conversion factors: 1 IU/l FSH = 1.5 nM FSH, 1 IU/l LH = 0.75 nM (Olivares *et al.*, 2000) and 1 IU/l hCG = 2.88 pM hCG (Stenman, 2004). We subsequently combined the measured LH and hCG concentrations as both proteins bind to the LH receptor with comparable affinity. As predicted by the model we find a much lower FSH and LH/hCG concentration in the follicular fluid compared with the serum (Fig. 6A and B).

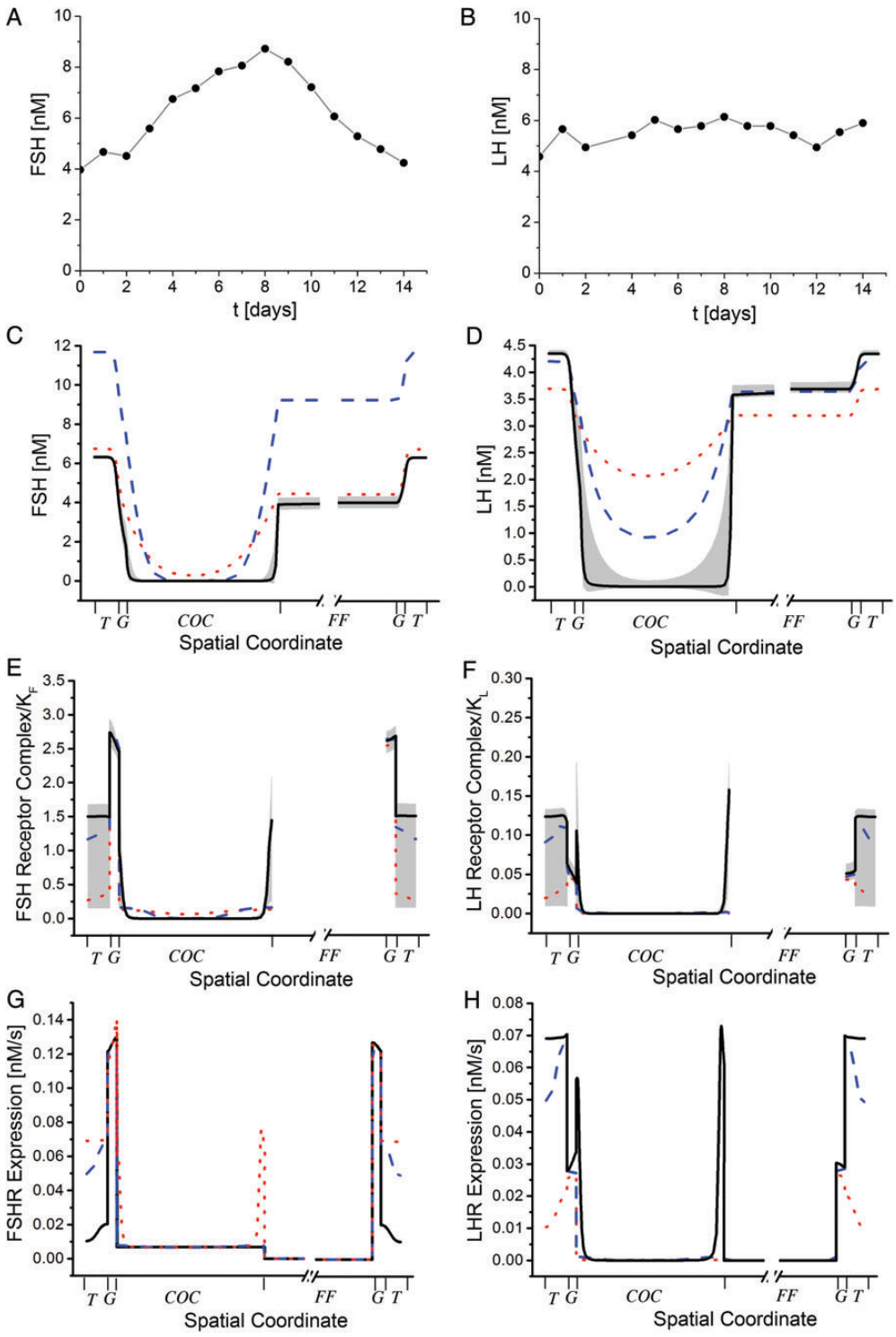

Figure 4 Dynamics of spatiotemporal signalling in the follicle. (**A** and **B**) Measured serum hormone concentrations of (A) FSH and (B) LH as reproduced from Brindle *et al.* (2006). The solid lines show the interpolations used in the simulations. (**C–F**) Simulated concentration profiles of (C) FSH, (D) LH, (E) FSH receptor complex and (F) LH receptor complex relative to their signalling thresholds K_F and K_L, and simulated (**G**) FSH receptor expression, and (**H**) LH receptor expression in the follicle. The three lines indicate three different time points: 2 (red, dotted), 6 (blue, dashed) and 14 days (black, solid lines). For a detailed discussion of the dynamics see the main text. The shaded areas in C–F indicate the standard deviation in the response at Day 14 when parameter values are sampled from a normal distribution with mean value as given in the Supplementary data, Table SI and standard deviation $\sigma = 0.1$. Note that all the simulations were carried out on a growing domain but are represented on a domain that is scaled such that all compartment sizes remain constant. The compartments on the horizontal axes indicate the different parts of the follicle, i.e. the theca (*T*), granulosa (*G*), COC (*COC*) and follicular fluid (*follicular fluid*). Note that in (C–H) only part of the follicular fluid domain is shown as the levels are constant within this domain.

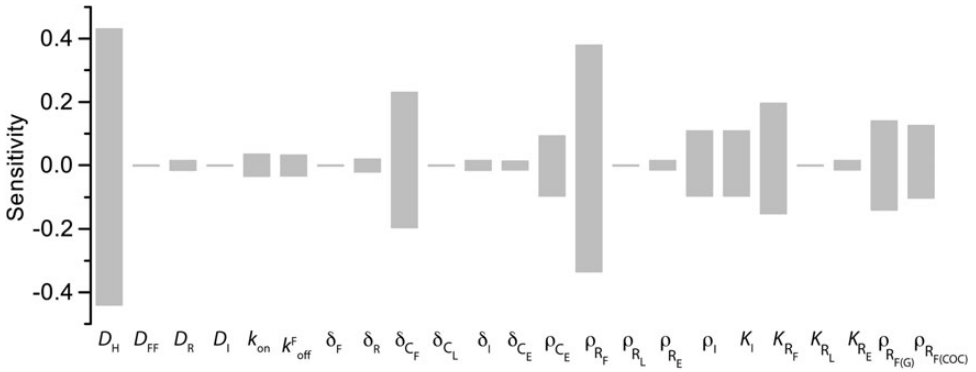

Figure 5 Sensitivity of the model output to changes in parameter values and initial conditions. Sensitivity of the relative FSH concentration in the follicular fluid and the serum to 1% changes in the kinetic parameter values; only parameters with a sensitivity coefficient >0.001 are shown.

During ovarian hyperstimulation the patients received different daily doses of FSH and LH, and we note that the differences between serum and follicular fluid concentrations decreases as the serum gonadotrophin levels increase (Fig. 6A and B). We checked whether we would obtain a similar saturation effect in the model, and we indeed obtain a similar result in the model (Fig. 6C and D). For ease of comparison we include the line that best fitted the experimental data in the simulation plots. This line (shown in black) aligns well with the simulated predictions (Fig. 6C and D, red dots).

Diffusion-based limits in granulosa cell layer thickness can explain scaling of follicle size with species weight

It has long been noticed that the size of follicles scales with the average species size (Table I, Fig. 7A) (Gosden and Telfer, 1987). It has been argued that this serves to increase the volume of the granulosa, and thus hormone production (Gosden and Telfer, 1987), but it has remained unclear why the volume of the granulosa would be increased via an expansion of the fluid-filled antrum rather than by a thickening of the granulosa layer. We used our parameterized model to explore the impact of increasing either the size of the fluid-filled antrum (as observed in nature) or the thickness of the granulosa on the estradiol production. When we analyse the estradiol production during follicle development relative to the surface area of the follicle (while keeping the thickness of the granulosa and the diameter of the COC constant) we observe a linear relationship (Fig. 7B, slope 0.991 ± 0.002, $R2 = 0.99996$), much as is observed in the differently sized species (Fig. 7A, slope 1.02 ± 0.08, $R2 = 0.885$). Assuming that heavier animals require more estrogens because their blood volume increases in parallel to body mass, the present analysis suggests that larger follicles can provide the required higher estradiol levels by accommodating more granulosa cells in the granulosa layer lining the follicular wall.

We next analysed the alternative option of increasing the thickness of the granulosa cell layer. We find that even if the thickness of the granulosa is strongly increased (while keeping the diameters of the follicle and of the COC constant), the total production of estradiol rises by at most 3-fold, because, as the thickness of the granulosa cell layer increases, insufficient gonadotrophins and androgen precursors reach the inner part of the granulosa layer, thereby limiting the activity of aromatase. A 10-fold decrease in granulosa thickness, on the other hand, reduces the estradiol concentration to almost zero (Fig. 7C). A further limitation in altering estradiol production via the granulosa thickness results from the follicular gonadotrophin concentration: a 4-fold increase in the thickness of the granulosa layer reduces the intra-follicular gonadotrophin concentration to almost zero, while a reduction in granulosa thickness doubles the follicular gonadotrophin concentration (Fig. 7C). There is therefore little room for the up-regulation of the estradiol production by increasing the granulosa thickness without affecting other processes. In summary, a higher rate of estradiol production, as is likely to be required by larger animals to achieve the same estradiol serum concentration at their higher blood circulation volumes, cannot be achieved by increasing the thickness of the granulose cell layer. Instead, their follicles need to become larger to accommodate more granulosa cells in a layer with similar thickness.

Gonadotrophins are sequestered by their receptors, and polymorphisms in the α-estrogen and the FSH-receptor genes have been associated with infertility (Perez Mayorga *et al.*, 2000; M'rabet *et al.*, 2012). The detailed biochemical impact of the changes in the FSH-receptor gene is not known but it has previously been noticed that reduction in binding capacity (NOT affinity) of LH- and FSH-receptor results in severe defects (Aittomäki *et al.*, 1995). While changes in the *LH-* and *FSH-receptor* expression levels have a much milder effect in the model than altering the granulosa cell layer thickness, a 10-fold change in receptor expression rates still raises the levels of FSH and of estradiol (but not of LH) in the follicular fluid by ~2-fold (Fig. 7D), thus potentially providing a mechanistic explanation for the observed clinical effects of the polymorphisms.

Finally, we note that variations in granulosa cell layer thickness within a species are likely to lead to disease as the hormone balance will be altered and the system is not self-correcting. Thus, a thicker granulosa layer will result in a reduced intra-follicular FSH concentration and a higher estradiol concentration; the higher estradiol concentration will down-regulate the release of FSH from the pituitary, thus further reducing the serum FSH concentration (Fig. 7C). Infertile women are often treated with exogenous FSH to stimulate ovarian function, thereby increasing the proliferation of granulosa cells and circulating levels of estradiol. We therefore tested whether the observed defects could be alleviated by adding FSH. To that end we increased and decreased the granulosa

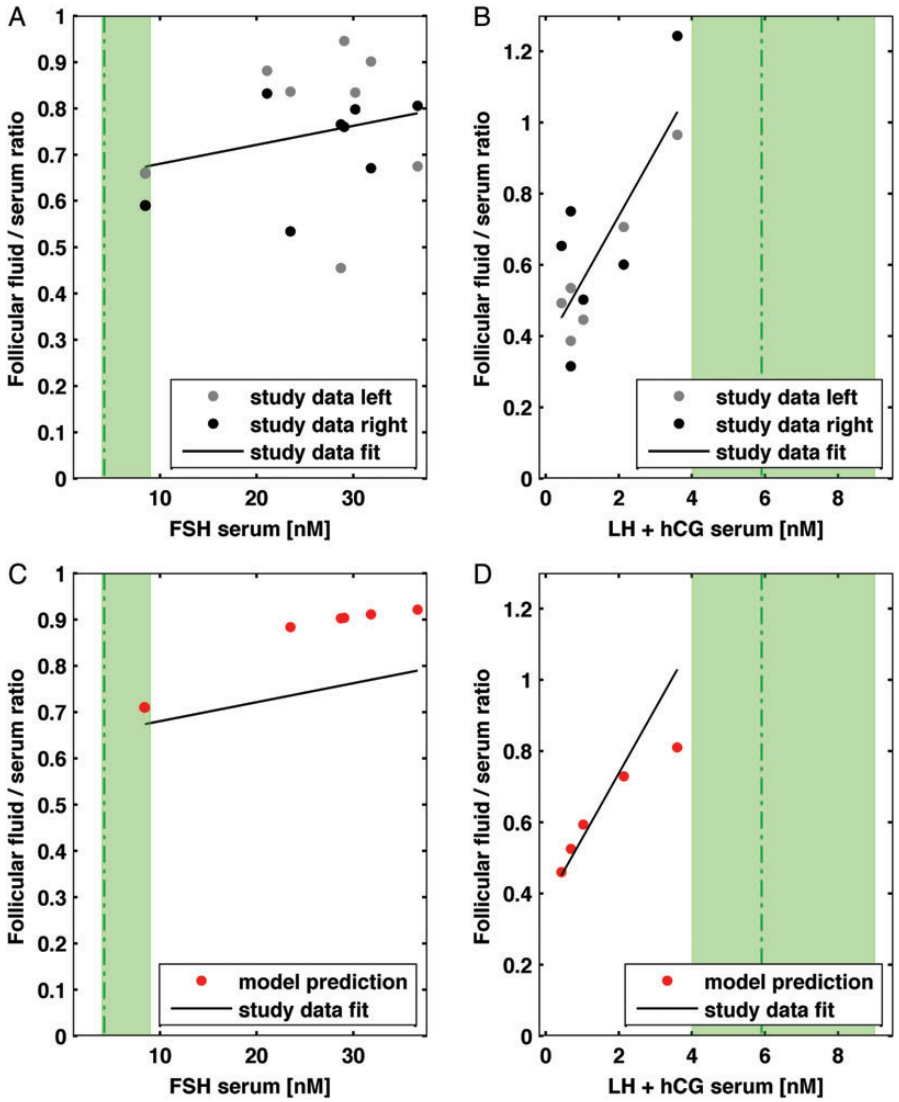

Figure 6 Predicted and experimentally confirmed FSH and LH gradients in the follicle. (**A** and **B**) The relative concentrations of (A) FSH, (B) hCG and LH in the follicular fluid and serum for different serum concentrations. Values < 1 indicate a lower gonadotrophin concentration in the follicular fluid. The data are based on measurements in the left and right ovary of eight patients undergoing assisted reproduction. For (B) only data of six patients could be used because in one patient the measured LSH concentration was below the detection limit. The fitted trend-line shows the dependency of the ratio on the gonadotrophin serum concentration. The shaded area (green) marks the physiological range of the serum concentrations used in the simulation based on the measured data in Fig. 4A and B, the vertical green, broken line represents the serum concentration at the last time point (14 days). The different ranges in Figs 4B and 6B is due to a mathematical conversion that takes into account the additional hCG in this panel here. (**C** and **D**) The model (red dots) predicts a gonadotrophin concentration difference between the serum and the follicular fluid. The extent of the difference depends on the serum concentration. The dependency obtained in the model is similar to the one observed in the data; the black trend line from the data in (A) and (B) is reproduced in (C) and (D) for ease of comparison. In the simulations constant serum levels were used over developmental time because at serum hormone levels were kept about constant in patients. Note that most of the patient serum hormone levels lie outside the physiological serum levels (green shaded area).

cell layer width and FSH concentrations in parallel (Fig. 7E). Raising the FSH-concentration in the serum compensates only for minor thickening of the granulosa. As the granulosa cell layer reaches 7-fold its normal thickness the gonadotrophin concentration in the follicular fluid (and thus in the enclosed COC) drops to negligible levels, even if additional external FSH is applied. In contrast, compensation by exogenous gonadotrophins would be successful in case of increased FSH-receptor expression levels (Fig. 7D).

Discussion

Growth of the ovarian follicle is mainly driven by the expansion of a fluid-filled cavity, the antrum. Follicular size is a key marker of successful follicular development, and sonographic measurement of follicular size is the single most reliable parameter for clinical decision-making in ovarian hyperstimulation. Despite its eminent importance in the monitoring of ovarian follicular growth, no direct role of the antrum has, however, so

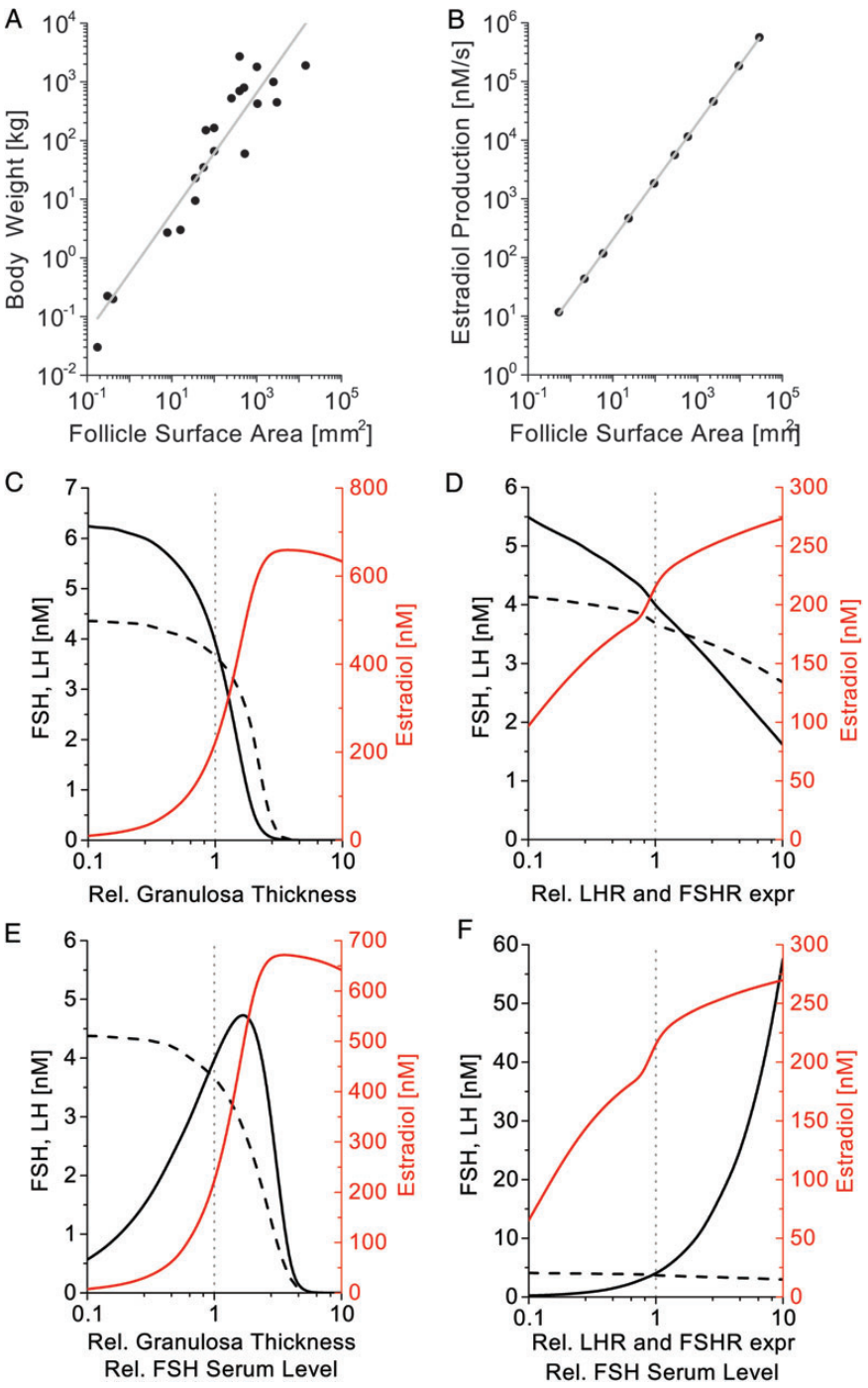

Figure 7 Diffusion-based limits in granulosa cell layer thickness can explain scaling of follicle size with species weight. (**A**) The follicle surface area correlates with the weight of mammalian species (Table I). (**B**) The rate of estradiol production of the mature follicle scales with the surface area of the mature follicle. Here only the volume of the antrum was increased; the thickness of the granulosa and the diameter of the COC was kept constant. (**C**–**F**) Receptor levels and granulosa width determine the extent of gonadotrophin sequestration in the granulosa. The average FSH (black solid line), LH (black, broken line) and estradiol (red) concentration in the follicular fluid at Day 14 (C) as the granulosa thickness is changed from its standard value denoted by 1, (D) as the *FSH-* and *LH-receptor* expression rates are changed from their standard value denoted by 1, (E) as both the granulosa thickness and the FSH serum levels are changed from their standard value denoted by 1, and (F) as both FSH serum levels and the *FSH-* and *LH-receptor* expression rates are changed from their standard value denoted by 1. Panels A and B were simulated on a constant 3D-domain of different radius as indicated. All other panels were simulated on growing domains.

far been identified and it is also an open question why the size of the antrum (and thus that of the follicle) differs to such an extent among different species.

By analysing published data on granulosa cell expansion and by computing the 4D-spatiotemporal events during follicular growth we demonstrate that the massive expansion of the follicle from a diameter of 5 mm–2 cm within 10–14 days is entirely driven by an increase of the volume of the follicular fluid, while the thickness of the granulosa cell layer remains constant at $\sim 45 \pm 10$ μm, even though granulosa cells strongly proliferate (Fig. 2). A similar thickness (~50 μm) of the granulosa cell layer has also been observed in other species, i.e. bovine (van Wezel *et al.*, 1999), goat and sheep (Mohammadpour, 2007). Based on the measured kinetic constants we predict that granulosa cells sequester gonadotrophins as they diffuse from the peripheral blood circulation into the follicular antrum (Figs 4 and 5) and we confirm the existence of a FSH- and LH-concentration gradient between the serum and the follicular fluid (Fig. 6). Based on these calculations, we conclude that a thicker granulosa cell layer would sequester and deplete important signalling factors, including FSH, delivered from the blood circulation towards the COC (Fig. 7).

The fluid-filled follicular antrum determines the surface area of the follicle and thereby the volume of the estrogen-secreting granulosa cell layer. In mono-ovulatory species, the appropriate serum concentration of estradiol is crucial for the selection of the dominant follicle through the fine tuning of the FSH secretion in the pituitary (Xu *et al.*, 1995). Due to their copious circulating blood volume, larger animals require the production of more estradiol and hence more granulosa cells to achieve the same modulatory effects in the pituitary. Increasing the size of the antrum in large animals allows for the expansion of the volume of the granulosa cell layer (and thus the production of more estrogens) without increasing the thickness of the granulosa cell layer.

In bovine follicles a thickness range of 40–100 μm has been reported for small antral follicles (diameter ~5 mm), and a much narrower range (close to 50 μm) for later stages of follicular development (van Wezel *et al.*, 1999). The observed variability may result from differences in cell shape and from an uncorrelated proliferation of granulosa cells and antrum expansion (Rodgers *et al.*, 2001). According to our model, a narrow range of thickness of the granulosa cell layer is important, because a thin granulosa cell layer would fail to produce sufficient amounts of estradiol to down-regulate FSH secretion in the pituitary, while a thicker granulosa cell layer, while producing more estradiol, would result in insufficient intra-follicular LH and FSH signalling due to limited diffusion (Fig. 7). In addition, higher estradiol levels would potentially prematurely lower the secretion of FSH by the pituitary and thereby additionally compromise the development of the oocyte in the COC. The small variability of granulosa cell layer thickness during the later stages of follicular development may thus derive from the sensitive impact of the estradiol-producing granulosa cell layer on the delicate balance between the acquisition of follicular dominance and atresia of follicles.

In assisted reproductive medicine, the addition of exogenous hormones during ovarian hyperstimulation not only increases the number of growing follicles but also raises the level of estradiol per mature follicle and the proliferation rate of the granulosa cells, in particular in those cases with high follicle numbers (De Geyter *et al.*, 1992; Attaran *et al.*, 1998; Gupta *et al.*, 2012). As a result, exaggerated thickening of the mural granulosa cell layer may block the diffusion of gonadotrophins and other hormones to the COC. During final follicular development, these constraints may be compensated to some extent by the increased formation of perifollicular capillaries. Interestingly, increased density of blood capillaries in the theca after wedge resection has been shown to revert the ovulatory function of polycystic ovaries due to enhanced delivery of FSH to the granulosa (Inzunza *et al.*, 2007). Moreover, earlier reports show that increasing the doses of gonadotrophins during ovarian hyperstimulation (step-up regimen) results in more collected oocytes (Christin-Maitre *et al.*, 2003), while lower numbers of oocytes are collected if the administration of FSH is withheld at the end of follicular development, as in prolonged coasting (D'Angelo *et al.*, 2011).

Data-based, validated computational models of biomedical processes are still rare, but they are likely to become invaluable tools to define the molecular causes of disease and to develop novel and individual therapeutic approaches that respect the complex regulatory logic of biological systems. Currently, in clinical reproductive medicine, the choice of the daily FSH dosage to be administered is exclusively based on a quantitative assessment of ovarian reserve, as given by the antral follicle count or the concentration of the anti-Muellerian hormone in the serum, but not on the FSH-receptor density or the capacity of the granulosa cells to proliferate. Mathematical models encompassing individual differences in receptor densities and activity may help to understand these effects in individual patients during ovarian hyperstimulation and perhaps assist in designing appropriate treatment modalities in each case prospectively.

Supplementary data

Supplementary data are available at http://molehr.oxfordjournals.org/.

Authors' roles

D.I. and C.D.G. designed the study; M.B., D.M. and D.I. carried out the analysis; D.I., C.D.G. and D.M. wrote the paper; all authors approved the final manuscript.

Funding

This work was supported by the Repronatal Foundation, Basel Switzerland.

Conflict of interest

None declared.

References

Adams GP, Singh J, Baerwald AR. Large animal models for the study of ovarian follicular dynamics in women. *Theriogenology* 2012;**78**:1733–1748.

Aerts JMJ, Bols PEJ. Ovarian follicular dynamics: a review with emphasis on the bovine species. Part I: Folliculogenesis and pre-antral follicle development. *Reprod Domest Anim* 2010;**45**:171–179.

Aittomäki K, Lucena JL, Pakarinen P, Sistonen P, Tapanainen J, Gromoll J, Kaskikari R, Sankila EM, Lehväslaiho H, Engel AR *et al.* Mutation in the follicle-stimulating hormone receptor gene causes hereditary hypergonadotropic ovarian failure. *Cell* 1995;**82**:959–968.

Assou S, Anahory T, Pantesco V, Le Carrour T, Pellestor F, Klein B, Reyftmann L, Dechaud H, De Vos J, Hamamah S. The human cumulus–oocyte complex gene-expression profile. Hum Reprod 2006;**21**:1705–1719.

Attaran M, Frasor J, Mascha E, Radwanska E, Rawlins RG. The relationship of human granulosa-lutein cell proliferative index to follicular diameter and serum estradiol. *Obstet Gynecol* 1998;**91**:449–453.

Aurich C. Reproductive cycles of horses. *Anim Reprod Sci* 2011;**124**:220–228.

Bao B, Garverick HA. Expression of steroidogenic enzyme and gonadotropin receptor genes in bovine follicles during ovarian follicular waves: a review. *J Anim Sci* 1998;**76**:1903–1921.

Bravo PW, Stabenfeldt GH, Lasley BL, Fowler ME. The effect of ovarian follicle size on pituitary and ovarian responses to copulation in domesticated South American camelids. *Biol Reprod* 1991;**45**:553–559.

Brindle E, Miller RC, Shofer JB, Klein NA, Soules MR, O'Connor KA. Urinary beta-luteinizing hormone and beta-follicle stimulating hormone immunoenzymometric assays for population research. *Clin Biochem* 2006;**39**:1071–1079.

Carin M. Numerical simulation of moving boundary problems with the ALE method: validation in the case of a free surface and a moving solidification front. In: *Excert from the Proceedings of the COMSOL Conference*, 2006.

Chiou CM, Yang TS, Yeh SP, Tsai MZ, Cheng SP, Huang MC. Changes in number of granulosa cells, follicular fluid levels and diameter of oocytes during folliculogenesis in pre-pubertal gilts at marketing weight. *Asian-Australasian J Anim Sci* 2004;**17**:1647–1651.

Christin-Maitre S, Hugues JN; Recombinant FSH Study Group. A comparative randomized multicentric study comparing the step-up versus step-down protocol in polycystic ovary syndrome. *Hum Reprod* 2003;**18**:1626–1631.

Couse JF, Yates MM, Deroo BJ, Korach KS. Estrogen receptor-beta is critical to granulosa cell differentiation and the ovulatory response to gonadotropins. *Endocrinology* 2005;**146**:3247–3262.

Cutress IJ, Dickinson EJF, Compton RG. Analysis of commercial general engineering finite element software in electrochemical simulations. *J Electroanal Chem* 2010;**638**:76–83.

D'Angelo A, Brown J, Amso MN. Coasting (withholding gonadotrophins) for preventing ovarian hyperstimulation syndrome. *Cochrane Database Syst Rev* 2011;CD002811.

De Geyter C, De Geyter M, Schneider HP, Nieschlag E. Interdependent influence of follicular fluid estradiol concentration and motility characteristics of spermatozoa on in-vitro fertilization results. *Hum Reprod* 1992;**7**:665–670.

Dhar A, Dockery P, O WS, Turner K, Lenton EA, Cooke ID. The human ovarian granulosa cell: a stereological approach. *J Anat* 1996;**188**:671–676.

Eppig JJ, Wigglesworth K, Pendola F, Hirao Y. Murine oocytes suppress expression of luteinizing hormone receptor messenger ribonucleic acid by granulosa cells. *Biol Reprod* 1997;**56**:976–984.

Erickson GF, Wang C, Hsueh AJ. FSH induction of functional LH receptors in granulosa cells cultured in a chemically defined medium. *Nature* 1979;**279**:336–338.

Evans ACO. Characteristics of ovarian follicle development in domestic animals. *Reprod Domest Anim* 2003;**38**:240–246.

Germann P, Menshykau D, Tanaka S, Iber D. Simulating organogensis in COMSOL. In: *Proceedings of COMSOL Conference*, Stuttgart, 2011.

Gloaguen P, Crépieux P, Heitzler D, Poupon A, Reiter E. Mapping the follicle-stimulating hormone-induced signaling networks. *Front Endocrinol* 2011;**2**:45.

Gosden RG, Telfer E. Scaling of follicular sizes in mammalian ovaries. *J Zool* 1987;**211**:157–168.

Gougeon A. Dynamics of follicular growth in the human: a model from preliminary results. *Hum Reprod (Oxford, England)* 1986;**1**:81–87.

Griffin J, Emery BR, Huang I, Peterson CM, Carrell DT. Comparative analysis of follicle morphology and oocyte diameter in four mammalian species (mouse, hamster, pig, and human). *J Exp Clin Assist Reprod* 2006;**3**:2.

Gupta C, Chapekar T, Chhabra Y, Singh P, Sinha S, Luthra K. Differential response to sustained stimulation by hCG & LH on goat ovarian granulosa cells. *Ind J Med Res* 2012;**135**:331.

Hermes R, Göritz F, Streich WJ. Assisted reproduction in female rhinoceros and elephants–current status and future perspective. *Reprod Domest Anim* 2007;**(Suppl. 2)**:33–44.

Hirakawa T, Minegishi T, Abe K, Kishi H, Ibuki Y, Miyamoto K. A role of insulin-like growth factor I in luteinizing hormone receptor expression in granulosa cells. *Endocrinology* 1999;**140**:4965–4971.

Iber D, De Geyter C. Computational modelling of bovine ovarian follicle development. *Bmc Syst Biol* 2013;**7**:60.

Iber D, Zeller R. Making sense-data-based simulations of vertebrate limb development. *Curr Opin Genet Dev* 2012;**22**:570–577.

Inzunza J, Morani A, Cheng G, Warner M, Hreinsson J, Gustafsson J-A, Hovatta O. Ovarian wedge resection restores fertility in estrogen receptor beta knockout (ERbeta-/-) mice. *Proc Natl Acad Sci USA* 2007;**104**:600–605.

Izumi T, Sakakida S, Muranishi Y, Nagai T. Allometric study on the relationship between the growth of ovarian follicles and oocytes in domestic cats. *J Reprod Dev* 2012;**58**:484–489.

Jeppesen JV, Kristensen SG, Nielsen ME, Humaidan P, Dal Canto M, Fadini R, Schmidt KT, Ernst E, Yding Andersen C. LH-receptor gene expression in human granulosa and cumulus cells from antral and preovulatory follicles. *J Clin Endocrinol Metab* 2012;**97**:E1524–E1531.

Kumar TR, Wang Y, Lu N, Matzuk MM. Follicle stimulating hormone is required for ovarian follicle maturation but not male fertility. *Nat Genet* 1997;**15**:201–204.

Lueders I, Taya K, Watanabe G, Yamamoto Y, Yamamoto T, Kaewmanee S, Niemuller C, Gray C, Streich WJ, Hildebrandt TB. Role of the double luteinizing hormone peak, luteinizing follicles, and the secretion of inhibin for dominant follicle selection in Asian elephants (Elephas maximus). *Biol Reprod* 2011;**85**:714–720.

Manjunatha BM, Pratap N, Al-Bulushi S, Hago BE. Characterization of ovarian follicular dynamics in dromedary camels (Camelus dromedarius). *Theriogenology* 2012;**78**:965–973.

McNatty KP. Hormonal correlates of follicular development in the human ovary. *Aust J Biol Sci* 1981;**34**:249–268.

Menshykau D, Iber D. Simulating organogenesis with comsol: interacting and deforming domains. In: *Proceedings of COMSOL Conference, Milano*, 2012.

Menshykau D, Kraemer C, Iber D. Branch mode selection during early lung development. *Plos Comput Biol* 2012;**8**:e1002377.

Minegishi T, Hirakawa T, Kishi H, Abe K, Abe Y, Mizutani T, Miyamoto K. A role of insulin-like growth factor I for follicle-stimulating hormone receptor expression in rat granulosa cells. *Biol Reprod* 2000;**62**:325–333.

Mohammadpour AA. Comparative histomorphological study of ovary and ovarian follicles in Iranian Lori-Bakhtiari sheep and native goat. *Pak J Biol Sci* 2007;**10**:673–675.

M'rabet N, Moffat R, Helbling S, Kaech A, Zhang H, de Geyter C. The CC-allele of the PvuII polymorphic variant in intron 1 of the α-estrogen receptor gene is significantly more prevalent among infertile women at risk of premature ovarian aging. *Fertil Steril* 2012;**98**:965–972.

Nair AK, Kash JC, Peegel H, Menon KMJ. Post-transcriptional regulation of luteinizing hormone receptor mRNA in the ovary by a novel mRNA-binding protein. *J Biol Chem* 2002;**277**:21468–21473.

Nakamura K, Liu X, Ascoli M. Seven non-contiguous intracellular residues of the lutropin/choriogonadotropin receptor dictate the rate of agonist-induced internalization and its sensitivity to non-visual arrestins. *J Biol Chem* 2000;**275**:241–247.

Olivares A, Cárdenas M, Timossi C, Zariñán T, Díaz-Sánchez V, Ulloa-Aguirre A. Reactivity of different LH and FSH standards and preparations in the world health organization matched reagents for enzyme-linked immunoassays of gonadotrophins. *Hum Reprod* 2000;**15**:2285–2291.

Osteen KG, Mills TM. Changes in the size, distribution and steroid content of rabbit ovarian follicles during early pseudopregnancy. *Biol Reprod* 1980; **22**:1040–1046.

Perez Mayorga M, Gromoll J, Behre HM, Gassner C, Nieschlag E, Simoni M. Ovarian response to follicle-stimulating hormone (FSH) stimulation depends on the FSH receptor genotype. *J Clin Endocrinol Metab* 2000; **85**:3365–3369.

Reynaud K, de Lesegno CV, Chebrout M, Thoumire S, Chastant-Maillard S. Follicle population, cumulus mucification, and oocyte chromatin configuration during the periovulatory period in the female dog. *Theriogenology* 2009;**72**:1120–1131.

Rhind SM, Bramley TA, Wright IA, McMillen SR. FSH and LH receptor concentrations in large ovarian follicles of beef cows in high and low levels of body condition at nine weeks post partum. *Reprod Fertil Dev* 1992;**4**:515–522.

Richards JS. Estradiol receptor content in rat granulosa cells during follicular development: modification by estradiol and gonadotropins. *Endocrinology* 1975;**97**:1174–1184.

Richards JS, Pangas SA. The ovary: basic biology and clinical implications. *J Clin Invest* 2010;**120**:963–972.

Richards JS, Russell DL, Ochsner S, Hsieh M, Doyle KH, Falender AE, Lo YK, Sharma SC. Novel signaling pathways that control ovarian follicular development, ovulation, and luteinization. *Recent Prog Horm Res* 2002; **57**:195–220.

Rodgers RJ, Irving-Rodgers HF. Formation of the ovarian follicular antrum and follicular fluid. *Biol Reprod* 2010;**82**:1021–1029.

Rodgers RJ, Irving-Rodgers HF, van Wezel IL, Krupa M, Lavranos TC. Dynamics of the membrana granulosa during expansion of the ovarian follicular antrum. *Mol Cell Endocrinol* 2001;**171**:41–48.

Sangha GK, Guraya SS. DNA, RNA and protein changes in rat ovarian follicles. In *Proc Indian Natn' Sci Acad B55 No 1989*.

Schwall RH, Erickson GF. Inhibition of synthesis of luteinizing hormone (LH) receptors by a down-regulating dose of LH. *Endocrinology* 1984; **114**:1114–1123.

Sharma SC, Clemens JW, Pisarska MD, Richards JS. Expression and function of estrogen receptor subtypes in granulosa cells: regulation by estradiol and forskolin. *Endocrinology* 1999;**140**:4320–4334.

Silva JM, Price CA. Insulin and IGF-I are necessary for FSH-induced cytochrome P450 aromatase but not cytochrome P450 side-chain cleavage gene expression in oestrogenic bovine granulosa cells in vitro. *J Endocrinol* 2002;**174**:499–507.

Simões J, Almeida JC, Valentim R, Baril G, Azevedo J, Fontes P, Mascarenhas R. Follicular dynamics in Serrana goats. *Anim Reprod Sci* 2006;**95**:16–26.

Singh J, Adams GP. Histomorphometry of dominant and subordinate bovine ovarian follicles. *Anat Rec* 2000;**258**:58–70.

Stenman U-H. Standardization of assays for human chorionic gonadotropin. *Clin Chem* 2004;**50**:798–800.

Stone BA, Serafini PC, Batzofin JH, Quinn P, Kerin JF, Marrs RP. Inter-relationships between plasma hormone levels and the content of total protein, gonadotropins and steroid hormones in antral fluids of women undergoing in vitro fertilization. *Fertil Steril* 1988;**50**:102–109.

Taneja M, Ali A, Singh G. Ovarian follicular dynamics in water buffalo. *Theriogenology* 1996;**46**:121–130.

Themmen AP, Blok LJ, Post M, Baarends WM, Hoogerbrugge JW, Parmentier M, Vassart G, Grootegoed JA. Follitropin receptor down-regulation involves a cAMP-dependent post-transcriptional decrease of receptor mRNA expression. *Mol Cell Endocrinol* 1991;**78**:R7–13.

Thummler V, Weddemann A. Computation of Space-Time Patterns via ALE Methods. In: *Proceedings of COMSOL Conference, Grenoble*, 2007.

van Wezel IL, Krupa M, Rodgers RJ. Development of the membrana granulosa of bovine antral follicles: structure, location of mitosis and pyknosis, and immunolocalization of involucrin and vimentin. *Reprod Fertil Dev* 1999;**11**:37–48.

Vetharaniam I, Peterson A, McNatty K. Modelling female reproductive function in farmed animals. *Anim Reprod* 2010;**122**:164–173.

Weddemann A, Thummler V. Stability analysis of ALE-methods for advection-diffusion problems. In: *Excert from the Proceedings of the COMSOL Conference, Hannover*, 2008.

Wood JR, Strauss JF. Multiple signal transduction pathways regulate ovarian steroidogenesis. *Rev Endocr Metab Disord* 2002;**3**:33–46.

Xu Z, Garverick HA, Smith GW, Smith MF, Hamilton SA, Youngquist RS. Expression of follicle-stimulating hormone and luteinizing hormone receptor messenger ribonucleic acids in bovine follicles during the first follicular wave. *Bio Reprod* 1995;**53**:951–957.

Zhou J, Kumar TR, Matzuk MM, Bondy C. Insulin-like growth factor I regulates gonadotropin responsiveness in the murine ovary. *Mol Endocrinol* 1997; **11**:1924–1933.